ELECTRICAL ENGINEERING AND ENERGY

OPEN ACCESS

Hybrid Adaptive MPPT Algorithm with Intelligent Exploration and Dither-Based Tracking for PV Systems

Hamzah Abdulkhaleq Naji[1]

[1] Iraqi Ministry of Education, Iraq

Submitted: 26 November 2025
Accepted: 20 December 2025
Online First:24 December 2025

Corresponding author
Hamzah Abdulkhaleq Naji
bcc0041@mtu.edu.iq

DOI:10.64470/elene.2025.1017

Abstract: This paper proposes an improved maximum power point tracking (MPPT) approach by developing a hybrid Perturb and Observe (P&O) and Incremental Conductance (INC) algorithm based on adaptive control, considering both existing influential perturbations, such as temperature and insolation changes, and integrating the kinks. The proposed method leverages P&O's fast decision-making capability for dynamic response and INC's slope estimation technique for higher precision around the maximum power point (MPP). Moreover, dither-gradient estimation and an adaptive exploration strategy are included to make the model more robust against noise and local maxima in partial shading. The controller works in two coordinated modes—Track and Explore—for achieving rapid convergence as well as steady-state stability. The oscillations are suppressed, and re-explorations can be made when the environment changes a lot, with a combination of dynamic reference power, exponential moving average (EMA) filtering, and irradiance-drop detection. The MATLAB/simulation results verified that the introduced hybrid P&O–Inc algorithm provides faster MPP tracking, better steady-state performance, and better tracking ability in PSC as well as under changing irradiances than other conventional detached MPPT methods.

Keywords: Adaptive Control, Global Maximum Power Point, Incremental Conductance, MPPT, Partial Shading, Photovoltaic, PV Systems, P&O.

1. Introduction

To get the most energy out of a photovoltaic (PV) array, one needs an MPPT controller that can reliably work at the single, ideal MPP on the nonlinear Power–Voltage curve (Saravanan & Babu, 2016). This point has the best conversion efficiency, but it moves around based on changes in solar irradiance and cell temperature. (Eze et al., 2024; Saravanan & Babu, 2016). Conventional methods, like P&O and INC, track the MPP by iteratively searching for the zero-slope condition ((Ahmad et al., 2022). However, these algorithms face a stability-speed trade-off: P&O oscillates at steady state (Saberi et al., 2023; Sonia et al., 2024)and is sluggish during transients, while INC is sensitive to noise. Critically, both fail under Partial Shading Conditions (PSC). Figure 1 illustrates the PV system integrated with an MPPT-controlled DC–DC boost converter. The MPPT controller regulates the converter's duty cycle through PWM to maintain the PV array's operation at or near the MPP under varying irradiance and temperature conditions, where the P-V curve produces multiple local maxima as shown in Figure 2 , potentially trapping the controller at a sub-optimal peak instead of the Global Maximum Power Point (GMPP) (Chowdhury et al., 2021). To

overcome these limitations. In recent years, numerous studies have focused on improving MPPT techniques for PV systems to enhance energy conversion efficiency under dynamic environmental conditions(Alshareef, 2025; Bakare et al., 2025; Bouksaim et al., 2025; Lamine et al., 2024; Naima et al., 2025; Wang et al., 2024). In light of these advancements, this work proposes a new Hybrid Adaptive MPPT controller based on a finite-state machine with two integrated modes (Iovino et al., 2025). The core design is an enhancement of classical gradient-based tracking, engineered for embedded real-time deployment with constant-time complexity and fixed-point–friendly arithmetic.

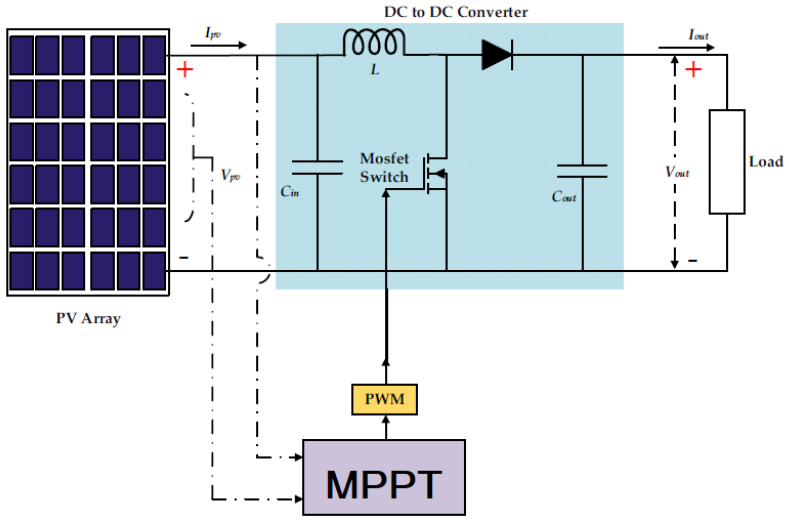

Figure 1 PV system with a DC–DC boost converter that is controlled by MPPT.

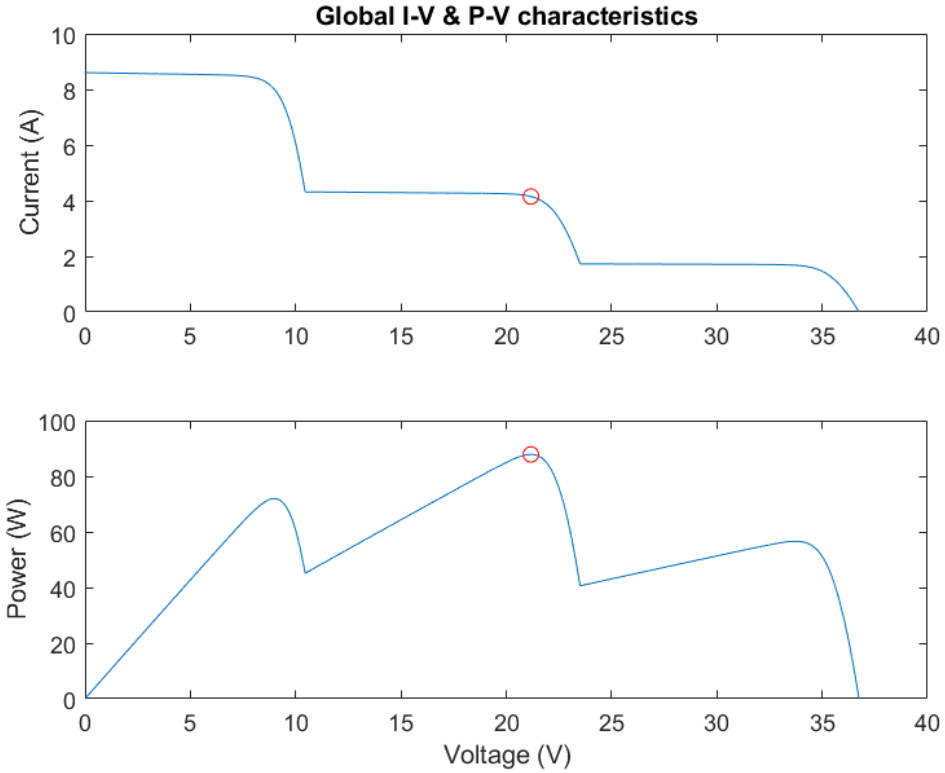

Figure 2 I–V and P–V characteristics of a PV array under partial shading showing multiple power peaks.

1. Track Mode (Stability and Noise Suppression): This is the high-efficiency steady-state mode. It applies a minuscule duty-cycle dither to infer only the sign of the power gradient ($\text{sign}(\partial P/\partial D)$) This conservative sign-based update minimizes oscillation. Stability is further enhanced by an EMA of measured power and a first-order output filter, which together effectively suppress sensor noise and switching ripple, achieving low ripple near the MPP without sacrificing responsiveness.
2. Exploratory Mode (PSC Resilience): This is a global search mode to improve MPPT robustness under irradiance transitions and partial shading conditions. It is triggered when the controller observes a steady deviation of power corresponding to a substantial isolation decrease. When activated, the algorithm uses a dithering-based perturbation with Kalman filter–assisted estimation to iterate toward the optimal duty ratio that is capable of tracking the new operating point well. The Kalman filter improves noise reduction and dynamic estimation of the power gradient, leading to accurate adjustment of tracking direction. This fast recovery after perturbations is made possible by the inclusion of this integration in the system, which minimizes oscillations and effectively identifies the global GMPP under complex partial shading scenarios.

The main contributions are in the hybrid FSM structure per se—a combination of high-precision filtered dithering and a Kalman filter–aided tracking MPPT method (Hajar et al., 2024)— that yields robust, low oscillations performance under uniform irradiance, while maintaining fast, reliable transients recovery and/or partial shading. The flowcharts of the P&O and INC MPPT techniques, which are proposed as two conventional benchmarking methods, are displayed in Figure 3. These figures illustrate the logical pathways that both algorithms use to chase the MPP, taking as input the changes in voltage and current.

2. Methodology

The proposed algorithm is conceptually inspired by the classical P&O (Azad et al., 2017) and INC methods (Safari & Mekhilef, 2011), combined with modern adaptive and extremum-seeking control principles (Leyva et al., 2006; Li et al., 2016; Mohapatra et al., 2019). From P&O, it inherits the simplicity and real-time suitability of perturbing the duty ratio and observing the corresponding power change, while from INC it adopts the analytical interpretation of the power–voltage slope, improving direction accuracy near the MPP. The method further incorporates elements of adaptive step-size and hybrid MPPT strategies, where two coordinated operating modes—Track for fine steady-state regulation and Explore for rapid re-localization after irradiance changes—are implemented in a finite-state framework. The integration of a decaying power reference and EMA smoothing follows adaptive control concepts for environmental change detection and noise suppression (Tajiri & Kumano, 2012). Meanwhile, the dither-based gradient estimation and localized bracket search are inspired by extremum-seeking control (Solís-Cervantes et al., 2024) and metaheuristic local-search techniques (Renaudineau et al., 2014), allowing efficient convergence to the global maximum even under partial shading.

2.1 Problem Formulation and Notation

At discrete control instants $k = 0,1,2,\ldots$, the PV array voltage and current are sampled as V_k and I_k. The instantaneous electrical power is

$$P_k = V_k * I_k \tag{1}$$

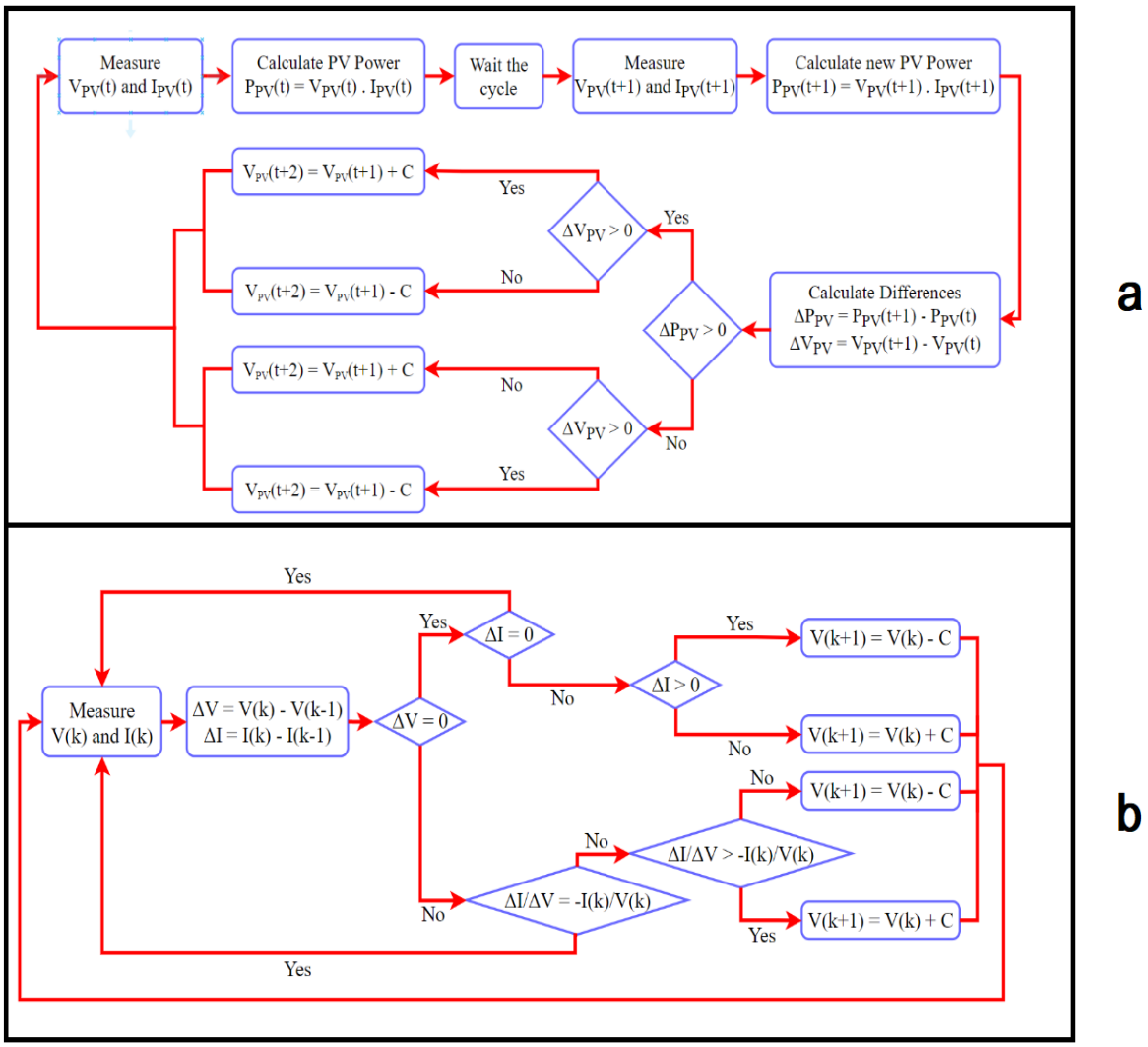

Figure 3 Flowcharts for the (a) (P&O) MPPT algorithm and the (b) INC MPPT algorithm. (Tozlu & Çalık, 2021).

The MPPT controller commands the duty ratio $u_k \in [d_{\min}, d_{\max}]$ of a DC–DC converter and maintains an internal (best) duty estimate d_k. The control objective is to drive u_k toward the power-maximizing duty

$$d^{\star} = \arg \max_{d \in [d_{\min}, d_{\max}]} P(d) \tag{2}$$

While achieving fast transients and low steady-state ripple. The algorithm uses: a small dithering amplitude $\delta > 0$; a gradient step $\eta > 0$; an exponential moving-average (EMA) gain $\alpha \in (0,1)$; a decaying power reference factor $\gamma \in (0,1)$; a drop threshold $\rho \in (0,1)$; sample-dwell counters; and a first-order output filter with coefficient $\beta \in (0,1)$.

2.2 Two-Mode Finite-State Architecture

The controller is a two-state FSM:

- Track (stability-oriented): estimate only the sign of $\partial P / \partial d$ using a small alternating dither and update d_k by clipped steps. A decaying power reference monitors for rapid irradiance changes.

- Explore (localized search): evaluate a small bracket of candidate duties around the current center, select the best performer, and shrink the bracket geometrically until stability is re-established, then return to Track.

Let c_k^{drop} count sustained power drops and c_k^{stable} count stable exploration sweeps. Transitions:

- Track → Explore when $c_k^{\text{drop}} \geq \theta_d$.
- Explore → Track when $c_k^{\text{stable}} \geq \theta_s$.

2.3 Noise Mitigation and Reference Signals

A light EMA is applied to power:

$$\tilde{P}_k \;=\; (1-\alpha)\,\tilde{P}_{k-1} \;+\; \alpha\,P_k, \quad \tilde{P}_0 = P_0 \tag{3}$$

A decaying peak reference tracks the recent maximum yet relaxes slowly:

$$R_k \;=\; \max\!\big(\gamma\,R_{k-1},\; \tilde{P}_k\big), \quad R_0 = P_0 \tag{4}$$

Equation (3) is a true EMA. Equation (4) is the non-decreasing (decaying peak) used for change detection; separating these two roles prevents bias and drift.

2.4 Environmental-Change (Irradiance-Drop) Detection

Define a drop event when the smoothed power falls sufficiently below the decaying reference:

$$\text{drop}_k \;=\; [\;\tilde{P}_k \;<\; (1-\rho)\,R_k\;]. \tag{5}$$

Use a robust counter (resets when the condition clears):

$$c_k^{\text{drop}} \;=\; \begin{cases} c_{k-1}^{\text{drop}} + 1, & \text{if } \text{drop}_k = 1, \\ 0, & \text{otherwise.} \end{cases} \tag{6}$$

When $c_k^{\text{drop}} \geq \theta_d$, declare an environmental change (e.g., irradiance step or partial shading) and enter Explore. This dual-threshold scheme (magnitude ρ and duration θ_d) screens out measurement noise yet reacts quickly to genuine changes.

2.5 Track Mode: Dither-Based Gradient-Sign MPPT

To avoid large perturbations, Track mode estimates only the **sign** of the power gradient using a tiny alternating dither:

$$\zeta_k \;=\; \delta\,(-1)^k, \qquad u_k^{\text{raw}} \;=\; \text{clip}(d_k + \zeta_k,\; d_{\min}, d_{\max}) \tag{7}$$

With a fixed ζ_k magnitude, a numerically stable gradient sign estimator is

$$g_k \;=\; \text{sign}((P_k - P_{k-1})\,\zeta_k) \tag{8}$$

Optionally guarded by a small $\varepsilon_P > 0$: if $|P_k - P_{k-1}| < \varepsilon_P$ then set $g_k = 0$. The best duty is nudged along g_k:

$$d_{k+1} \;=\; \text{clip}(d_k + \eta\,g_k,\; d_{\min}, d_{\max}) \tag{9}$$

To temper jitter and enforce actuator bandwidth limits, apply a first-order output filter:

$$u_k \;=\; (1-\beta)\,u_{k-1} \;+\; \beta\,d_k, \qquad u_0 = d_0 \tag{10}$$

Equations (7)– (10) realize a low-oscillation, sign-only MPPT update that is code-generation friendly and robust to quantization.

2.6 Explore Mode: Localized Bracketing and Adaptive Shrink

Upon an environmental change, initialize a symmetric bracket around the current center $d_c = d_k$ with inner and outer half-widths $w_{\text{in}}, w_{\text{out}} > 0$:

$$C_k = \text{clip}(d_c - w_{\text{out}}), \text{clip}(d_c - w_{\text{in}}), \text{clip}(d_c + w_{\text{in}}), \text{clip}(d_c + w_{\text{out}}) \quad (11)$$

Each candidate $c \in C_k$ is applied for τ controller ticks (short dwell) to allow settling; record its best measured (or EMA-smoothed) power

$$\hat{P}(c) = \max_{t \in (1,\ldots,\tau)} \tilde{P}_{k+t} \text{ at } u = c \quad (12)$$

Select the winner and re-enter:

$$c^\star = \text{argmax}_{c \in C_k} \hat{P}(c), \qquad d_{k+\tau} = c^\star \quad (13)$$

Shrink the bracket geometrically to "lock in" as improvements taper:

$$w_{\text{in}} \leftarrow \kappa\, w_{\text{in}}, \qquad w_{\text{out}} \leftarrow \kappa\, w_{\text{out}}, \qquad 0 < \kappa < 1 \quad (14)$$

Increase a stability counter c_k^{stable} when the winner remains consistent (or improvements fall below a slack threshold). When $c_k^{\text{stable}} \geq \theta_s$, return to Track and resume fine dithering around the new optimum neighborhood.

2.7 Parameterization and Safe Defaults

Typical, hardware-friendly defaults that balance agility and ripple (tune per system bandwidth and sensor noise):

- Saturation: $d_{\min} = 0.05,\ d_{\max} = 0.95$.
- Dither amplitude: $\delta \in [10^{-3}, 3 \times 10^{-3}]$
- Gradient step: $\eta \in [10^{-3}, 5 \times 10^{-3}]$
- EMA gain (power): $\alpha \in [0.05, 0.2]$.
- Decaying reference: $\gamma \in [0.990, 0.997]$
- Drop threshold/duration: $\rho \in [0.04, 0.08]$, $\theta_d \in (3, \ldots, 8)$.
- Explore dwell: $\tau \in (4, \ldots, 12)$ ticks; shrink $\kappa \in [0.5, 0.7]$; stability $\theta_s \in (1,2,3)$.
- Output filter (duty): $\beta \in [0.1, 0.3]$.
- Safety guards: $\varepsilon_P \approx 10^{-4}$–$10^{-3}$ p.u.; clip all duties with $\text{clip}(\cdot)$.

Reference Defaults at a Glance

$$\delta = 0.001 - 0.003,\ \eta = 0.002,\ \alpha = 0.1,\ \beta = 0.2,\ \gamma = 0.995,$$
$$\rho = 0.06,\ \tau = 8,\ \kappa = 0.6,\ \theta_d = 5,\ \theta_s = 2,\ T_s = 2\,\text{ms}.$$

2.8 Behavior Under Partial Shading

Under partial shading, $P(d)$ becomes multimodal. The Explore phase performs a compact, four-point local scan with adaptive bracketing. By re-centering on the empirically best candidate and shrinking the bracket, the controller escapes inferior local maxima and quickly restores Track operation around the new neighborhood of the global (or dominant) MPP. The operational logic of the proposed hybrid adaptive

MPPT controller is illustrated in Figure 4**,** which outlines the transition between the ***exploration*** and ***tracking*** stages governed by the FSM framework. The detailed algorithmic sequence corresponding to this flow is presented in Table 1, summarizing the simplified pseudocode steps executed within the controller.

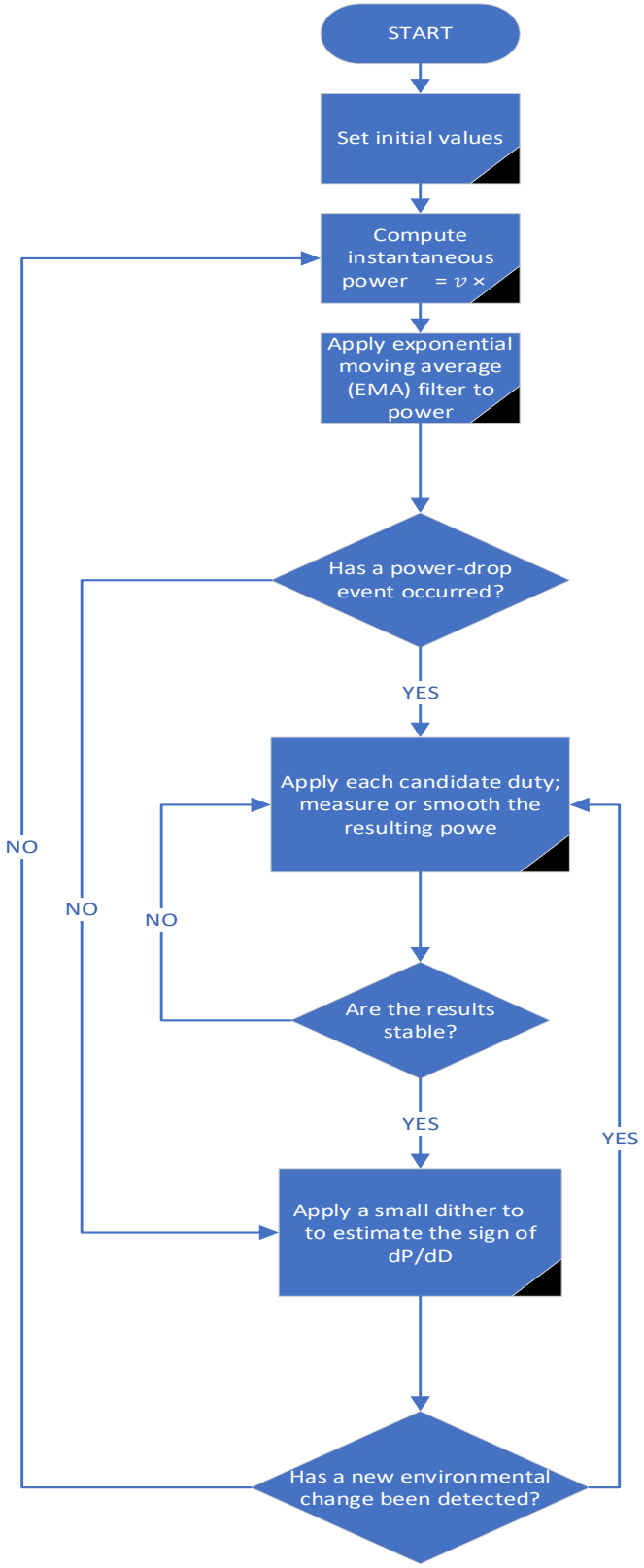

Figure 4 Flowchart of the proposed hybrid adaptive MPPT algorithm combining exploration and tracking stages.

Table 1 Simplified Pseudocode Steps of the Proposed Hybrid MPPT Algorithm

Step	Current State	Main Condition	Action / Operation	Next State
1	Start / Init	First run	Initialize all constants and memory: D=0.5, D_{best}=D, set limits, counters, and parameters.	Track
2	Track	Normal operation, no power drop	Compute P = V * I; estimate gradient sign ($\left(\frac{dP}{dD}\right)$ update D_{best}: $D_{best} = D_{best} + K_{grad} * \text{sign}\left(\frac{dP}{dD}\right)$; apply small dither; smooth duty output.	Track
3	Track → Explore	If power falls below the reference for several samples (dropCnt > threshold)	Switch to *Explore*; set 4 nearby duty candidates around the best D.	Explore
4	Explore	Scan each candidate's D_i	Apply each candidate's duty, record its measured power P_i, keep the maximum.	Explore
5	Explore evaluation	After all candidates had tested	Select the best candidate, $D_{best} =, D_{best}$; shrink the search range around it; update counters.	Explore or Track
6	Explore → Track	If the system is stable (stableSweep ≥ limit)	Return to *Track* mode; reset counters.	Track
7	End / Output	Always	Output final duty cycle D to the converter.	Return

3. Modeling and Simulation

The proposed hybrid MPPT algorithm is evaluated under three operating scenarios to assess its accuracy, dynamic response, and robustness: Case 1, the Standard Test Condition (1000 W/m²); Case 2, dynamic performance under variable irradiance; and Case 3, performance evaluation under partial shading conditions. The simulation and modeling phase were conducted in MATLAB/Simulink to analyze the performance of the developed MPPT algorithms with various irradiance conditions. The system as a whole includes three primary subsystems: the PV array model, the DC–DC boosting power converter, and the MPPT control section. The PV array includes three photovoltaic panels in series connection, each of the panels being supplied with a different irradiance level to represent partial shading conditions. The irradiance inputs were provided as time step signals that are time-variant to represent different intensities of sunshine, with the cell temperature being maintained as a fixed value of 25 °C. The PV module is represented by the single-diode model that is correct in depicting the nonlinear current–voltage characteristic as a function of irradiance as well as temperature. The DC–DC booster conversion interface connects the PV module with the load and is held to be in control of the operating duty voltage based on the duty cycle set from the MPPT controller. Through this modeling framework, the system's transient and steady-state behaviors are analyzed under various irradiance patterns, enabling a fair comparison between the adaptive hybrid MPPT in terms of convergence speed, ripple minimization, and tracking efficiency, as shown in Figure 5 and Figure 6.

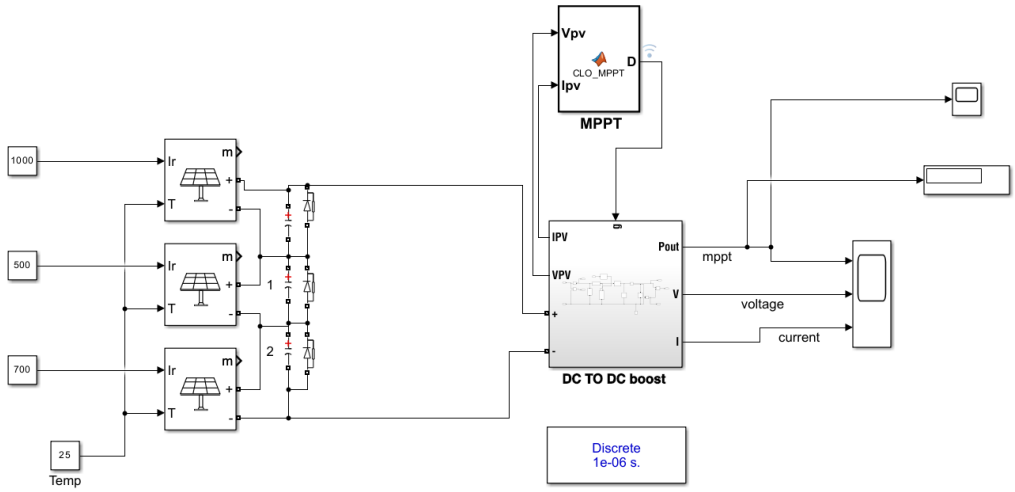

Figure 5 Simulink model of a photovoltaic system

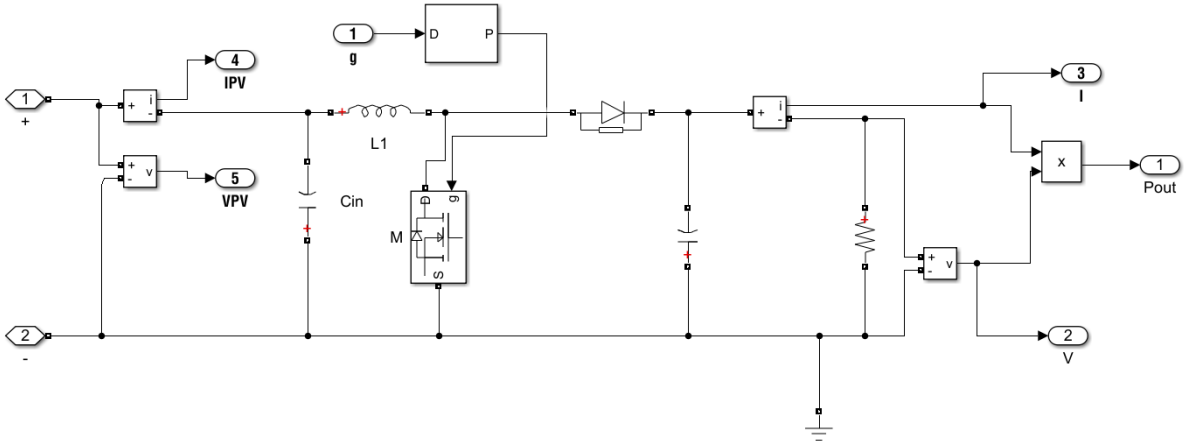

Figure 6 Simulink schematic of the DC–DC boost converter

The performance characteristics of the boost converter are defined by the following key parameters: a switching frequency (f_s) of 5000 Hz, and a duty cycle (which modulates the ratio of the switch-on time to the total switching period. The converter utilizes a MOSFET with an internal on-resistance (R_{on}) of 1×10^{-3} Ω and a diode specified with an internal resistance (R_d) of 1×10^{-3} Ω, a forward voltage (V_f) of zero, and zero internal inductance (L_{on}). The primary figures of merit monitored are the output voltage (V_{out}) and output current (I_{out}), which are used to calculate the converter's output power ($P_{out} = V_{out} \cdot I_{out}$).also The parameters of PV array can be shown in Figure 7.

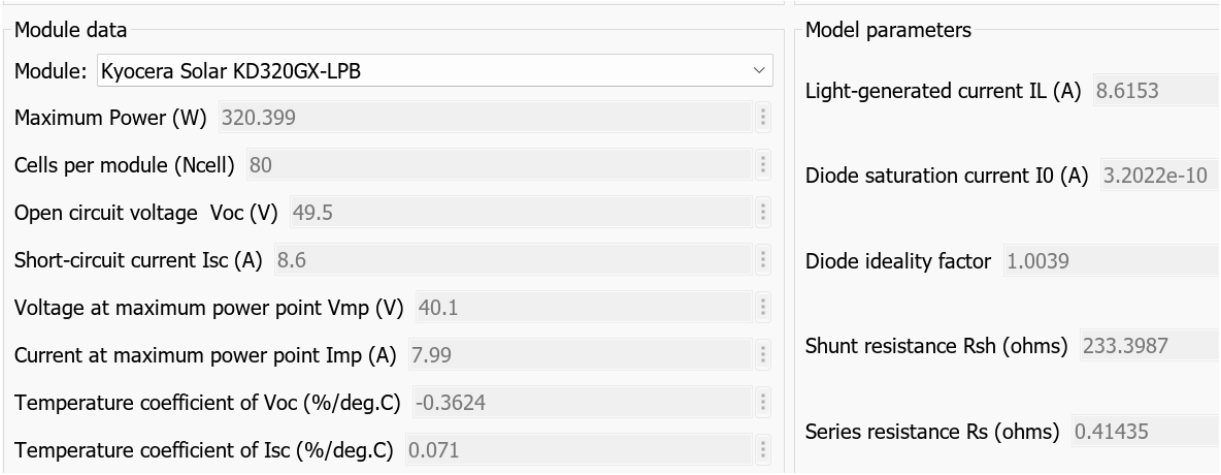

Figure 7 PV array parameters

4. Results and Discussion

4.1 Results

Case 1: Standard Test Condition

Figure 8 shown the simulation output and how the proposed hybrid MPPT controller works in both dynamic and steady-state conditions. The power curve exhibits a rapid rise from zero to approximately 900–950 W within about 0.15 s, followed by a stable plateau with negligible oscillations. This indicates that the algorithm successfully locates and maintains operation at the MPP with minimal steady-state error. The smooth convergence and absence of overshoot demonstrate effective damping and appropriate gain selection in the duty-ratio adaptation. Furthermore, the small ripple amplitude (< 1%) around the steady-state value confirms the efficiency of the dither-based filtering and exponential moving average smoothing mechanisms integrated into the controller, as shown in and Table 2.

Table 2 MPPT Performance under Standard Test Condition (1000 W/m²)

Parameter	Observed Result
Convergence Time	≈ 0.15 s
Steady-State Power	≈ 900–950 W
Oscillation Amplitude	< 1% of the mean power
Tracking Efficiency	≈ 98–99% (estimated)
System Stability	No overshoot, smooth settling

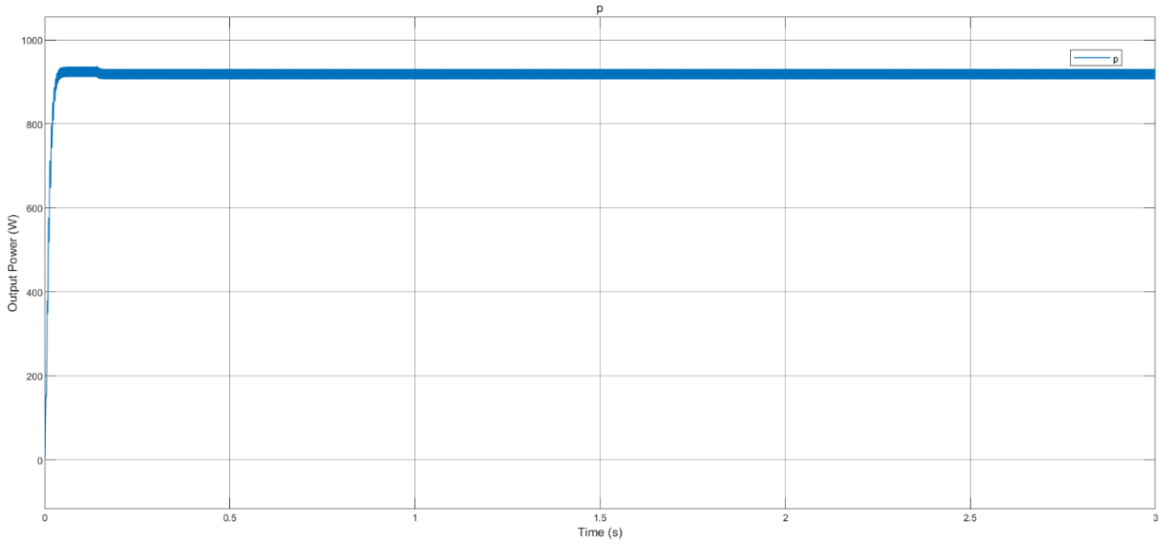

Figure 8 PV output power response under uniform irradiance (STC: 1000 W/ m²).

Case 2: MPPT Dynamic Performance under Variable Irradiance

Figure 9 shows the presented power–time plots illustrate the dynamic response of the proposed hybrid MPPT algorithm under rapid irradiance changes. Initially, the output power increases sharply and stabilizes near 250–300 W, followed by two-step transitions corresponding to irradiance rises and drops as shown in Table 3. The first transient (around 1 s) shows a quick rise to approximately 500 W, while the subsequent irradiance reduction (around 1.4–1.5 s) results in a smooth decline and stabilization near 400 W. Throughout these transitions, the algorithm maintains fast tracking and strong disturbance rejection without significant overshoot or oscillatory instability.

Table 3 Solar Cell Irradiance over Time

Time (s)	Cell 1 Irradiance (W/m²)	Cell 2 Irradiance (W/m²)	Cell 3 Irradiance (W/m²)
0.0	800	500	200
0.5	500	300	600
1.0	300	800	900
1.5	1000	600	300

The short transient deviation and fast re-settling (< 0.1s) are indicative of efficient switching between the Track and Explore modes, which allows the controller to quickly sense changes in the environment, but also respond to them as soon as possible. The continuous, rapid plateauing passages following each irradiance event justifies the robustness and adaptability of the hybrid sensor early warning structure, alongside the reliability of its irradiance drop detection logic discussed in this paper, as depicted in Table 4.

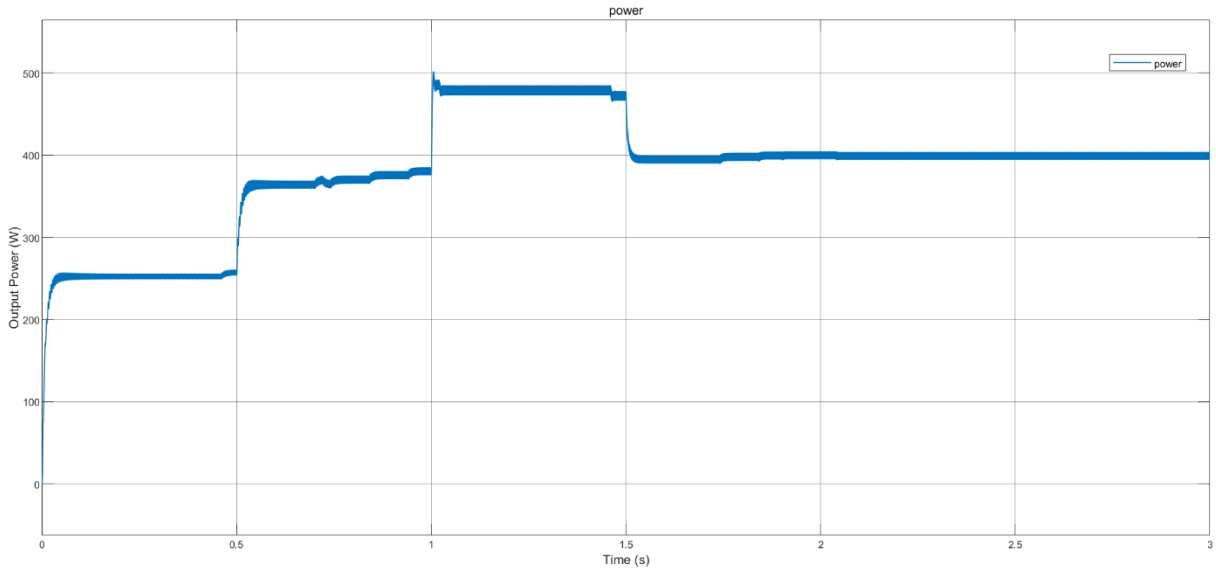

Figure 9 MPPT performance of the PV system under step-change irradiance (Case 2)

Table 4 MPPT Performance under Step Changes in Irradiance (Case 2)

Performance Metric	Observed Value / Behavior	Interpretation
Tracking Speed	< 0.1 s after each irradiance change	Very fast response; efficient dynamic tracking
Power Transition Levels	≈ 250 → 500 → 400 W	Accurate response to irradiance increases and decreases
Overshoot / Undershoot	Negligible	Well-damped transient, stable control
Steady-State Ripple	< 1–2 %	Low oscillation, strong filtering effect
Mode Switching Performance	Smooth transitions between Track/Explore	Effective irradiance-drop detection and adaptive control

Case 3: MPPT Performance Evaluation under Partial Shading Conditions

Figure 10 shows the graphs representing the transient and steady-state performance of the proposed hybrid MPPT controller when subjected to partial shading variations. The first figure shows the global tracking response, where the output power initially stabilizes around 360–370 W, then progressively climbs to approximately 400 W as the algorithm identifies and locks onto the GMPP in PSC (1000-300-600) W/ m². This gradual stepwise improvement indicates the controller's exploration phase effectively scanning local maxima and converging to the global optimum with no overshoot or oscillatory instability. The second, zoomed-in plot reveals a very small periodic oscillation around the final power level (≈ ±5 W), corresponding to the algorithm's fine dithering in Track mode, which maintains the system near the MPP with minimal steady-state ripple. The overall response demonstrates excellent dynamic performance, low power fluctuation, and strong robustness under nonuniform irradiance, as shown in and Table 5.

Table 5 MPPT result of the PV system under partial shading conditions (Case 3)

Performance Metric	Observed Behavior / Value
Initial Tracking Time	≈ 0.2 s
Global Peak Acquisition	Achieved around t = 1.8 s
Steady-State Power	≈ 400 W
Ripple Amplitude	≈ ±5 W (< 1.5 %)
Overshoot / Undershoot	None
Adaptation to Partial Shading	Effective

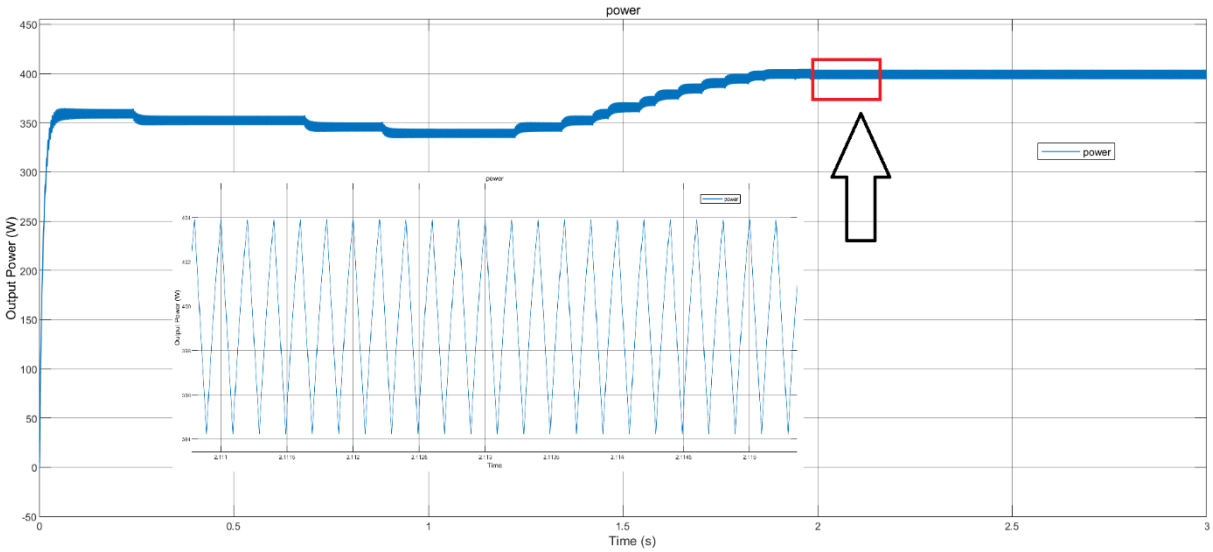

Figure 10 MPPT performance of the PV system under partial shading conditions (Case 3)

Case 4: Performance comparison under PSC

The performance of the proposed method was analyzed against several known algorithms under the exact same operating conditions, partial shading, specifications, and time durations. Figure 11 shows that the other algorithms became stuck at a local peak, while the proposed method was able to bypass local peaks and move towards the global peak. A different radiation was applied to each of the three cells, with the same intensity as in case 3 (1000, 300, 600) W/ m². The intensity at which the method stuck was recorded and compared with the others. The recorded values can be seen in Table *6* .

Table 6 Steady-State Performance Summary of MPPT Algorithms Under Partial Shading

Algorithm	Steady State Power (Watt)	Peak Type Achieved	Key Performance Observation
HYBRID (Proposed)	~ 400 W	Global Peak	Highest efficiency; successfully tracks the maximum available power.
INC	~ 360 W	Local Peak	Fast convergence but stuck at LP
P&O	~ 325 W	Local Peak	Good stability but poor efficiency due to trapping at a lower LP.
CS	~ 290 W	Local Peak	Lowest power yield among the compared algorithms.
GWO	~ 324 W	Local Peak	Shows large initial fluctuations (overshoot).

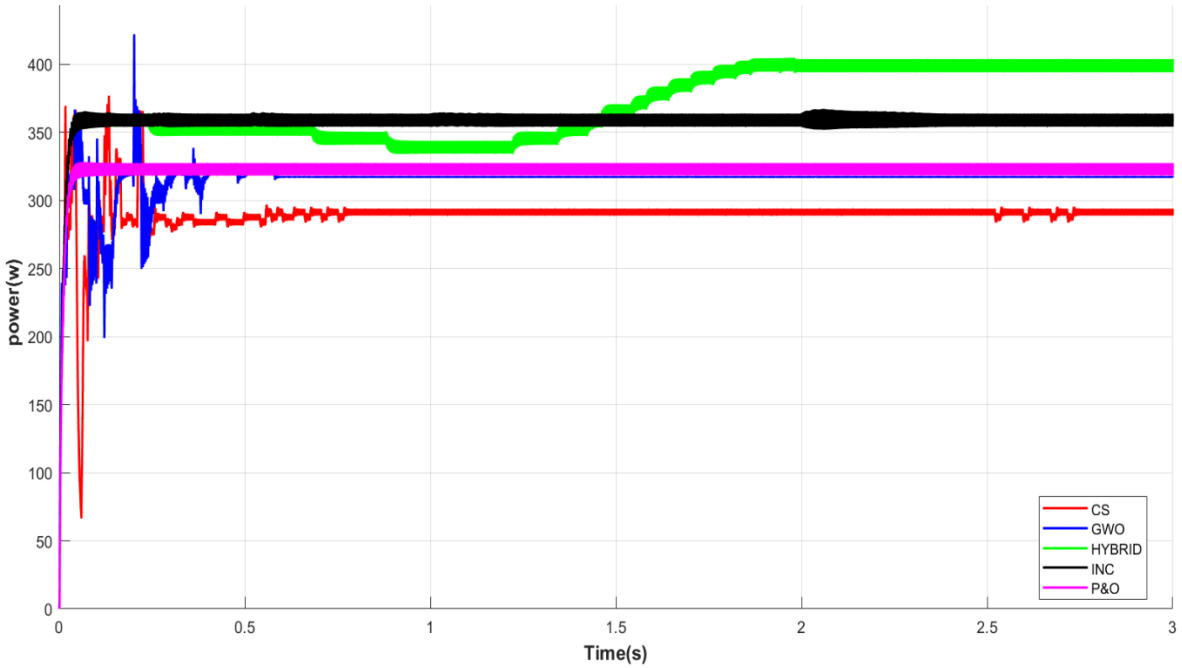

Figure 11 Performance Comparison of Various MPPT Algorithms Under Partial Shading Conditions

The figure clearly illustrates the performance comparison of five MPPT algorithms under identical partial shading conditions. The primary challenge in this scenario is the presence of multiple peaks in the power-voltage curve, where traditional methods often get trapped at a Local Peak (LP) instead of reaching the Global Peak (GP). The HYBRID (Proposed) method, represented by the green line, is the only algorithm that successfully bypasses the LPs and settles robustly at the GP, achieving approximately 400 W after an initial convergence time of about 1.8 seconds. In contrast, conventional methods like INC and P&O demonstrated faster initial response (under 0.5s) but became permanently stuck at LPs, yielding significantly lower power outputs of around 360 W and 325 W, respectively. Furthermore, the INC algorithm exhibits high steady-state oscillations, indicated by the thick black line, demonstrating poorer stability compared to the smooth curves of P&O and HYBRID. This confirms that the proposed HYBRID strategy provides a substantial power gain—approximately 11% higher than the INC method—making it superior in terms of efficiency and resilience against partial shading effects.

4.2 Discussion

The simulation results show that the hybrid MPPT algorithm is equally applicable to normal or non-uniform irradiance input environments. The controller has the properties of rapid convergence and smooth transient response with small steady state oscillation, especially when the irradiance rapidly changes. Thanks to the adaptive Track/Explore mechanism, irradiance drops are quickly detected, and the global GMPP is relocated in just a about 0.1 second, which surpasses both classical P&O and INC approaches in terms of speed and robustness. The algorithm differentiates between local and global peaks well in partial shading cases, showing that it can appropriately track the true MPP continuously with little power loss. As against metaheuristic strategies, for instance, PSO, the optimized hybrid algorithm leads to the same final power levels with faster control responses and lower computational load, placing it closer to real-time embedded PV systems. In general, the results verify that the proposed approach is robust enough and able to work very well in dynamic operational conditions.

5. Conclusions

The proposed hybrid adaptive MPPT algorithm significantly improves the efficiency of photovoltaic energy conversion by combining dither-based gradient tracking with an intelligent exploration mechanism. This novel approach ensures rapid and accurate tracking of the MPP under both uniform irradiance and partial shading conditions. The ability to seamlessly switch between the Track and Explore modes allows the algorithm to quickly adapt to changes in environmental conditions, reducing oscillations and ensuring stability. Moreover, the integration of power-drop detection, exponential smoothing, and adaptive bracketing further enhances system performance, making it more reliable and resilient in real-time applications. Simulation results confirm that the proposed method outperforms traditional Perturb and Observe (P&O) and Incremental Conductance (INC) algorithms in terms of speed, accuracy, and stability, while maintaining computational efficiency. This makes it a promising solution for real-time MPPT applications in PV systems, particularly in environments with fluctuating irradiance and partial shading conditions.

Declaration of Ethical Standards

As the author of this study, I declare that it complies with all ethical standards.

Credit Authorship Contribution Statement

Hamzah Abdulkhaleq Naji: Writing -Original Draft, Visualization, Methodology, Investigation, Resources, Writing, Review & Editing.

Declaration of Competing Interest

The author declared that he has no conflict of interest.

Funding / Acknowledgements

The author declare that no specific funds or grants were received from any public, commercial, or not-for-profit agencies during the preparation of this work. The author would like to express their sincere gratitude to Mr. Hassan Safy Ahmed for his valuable support and assistance in this work.

Data Availability

No datasets were generated or analyzed during the current study.

References

Ahmad, M. E., Numan, A. H., & Mahmood, D. Y. (2022). A comparative study of perturb and observe (P&O) and incremental conductance (INC) PV MPPT techniques at different radiation and temperature conditions. *Eng. Technol. J*, 40(2), 376-385. https://doi.org/http://doi.org/10.30684/etj.v40i2.2189

Alshareef, M. J. (2025). An enhanced fractional open circuit voltage MPPT method for rapid and precise MPP tracking in standalone photovoltaic systems. *IEEE Access*. https://doi.org/https://doi.org/10.1109/ACCESS.2025.3543327

Azad, M. L., Das, S., Sadhu, P. K., Satpati, B., Gupta, A., & Arvind, P. (2017). P&O algorithm based MPPT technique for solar PV system under different weather conditions. 2017 *International Conference on Circuit, Power and Computing Technologies (ICCPCT)*,

Bakare, M. S., Abdulkarim, A., Shuaibu, A. N., & Muhamad, M. M. (2025). Enhancing solar power efficiency with hybrid GEP ANFIS MPPT under dynamic weather conditions. *Scientific Reports*, 15(1), 5890. https://doi.org/https://doi.org/10.1038/s41598-025-90417-1

Bouksaim, M., Mekhfioui, M., & Srifi, M. N. (2025). A Comprehensive Decade-Long Review of Advanced MPPT Algorithms for Enhanced Photovoltaic Efficiency. Solar,

Chowdhury, S. B. R., Mukherjee, A., & Gayen, P. K. (2021). Maximum power point tracking of photovoltaic system by Perturb & Observe and Incremental Conductance methods under normal and partial shading conditions. 2021 *Innovations in Energy Management and Renewable Resources* (52042),

Eze, V. H. U., Richard, K., Ukagwu, K. J., & Okafor, W. (2024). Factors Influencing the Efficiency of Solar Energy Systems. *Journal of Engineering, Technology, and Applied Science (JETAS)*, 6(3), 119-131. https://doi.org/https://doi.org/10.36079/lamintang.jetas-0603.748

Hajar, A., Ahmed, G., Youness, H., & Benachir, E. H. (2024). Optimizing photovoltaic system efficiency through a Kalman filter driven approach for MPPT in partial shading conditions. *2024 4th International Conference on Innovative Research in Applied Science, Engineering and Technology (IRASET)*,

Iovino, M., Förster, J., Falco, P., Chung, J. J., Siegwart, R., & Smith, C. (2025). Comparison between behavior trees and finite state machines. *IEEE Transactions on Automation Science and Engineering*. https://doi.org/https://doi.org/10.1109/TASE.2025.3610090

Lamine, O. M., Bessous, N., Abdelhalim, B., Banakhr, F. A., Mosaad, M. I., Oussama, M., & Mahmoud, M. M. (2024). A Combination of INC and Fuzzy Logic-Based Variable Step Size for Enhancing MPPT of PV Systems. *International Journal of Robotics & Control Systems,* 4(2). https://doi.org/http://dx.doi.org/10.31763/ijrcs.v4i2.1428

Leyva, R., Alonso, C., Queinnec, I., Cid-Pastor, A., Lagrange, D., & Martinez-Salamero, L. (2006). MPPT of photovoltaic systems using extremum-seeking control. *IEEE transactions on aerospace and electronic systems*, 42(1), 249-258. https://doi.org/https://doi.org/10.1109/TAES.2006.1603420

Li, C., Chen, Y., Zhou, D., Liu, J., & Zeng, J. (2016). A high-performance adaptive incremental conductance MPPT algorithm for photovoltaic systems. Energies, 9(4), 288. https://doi.org/https://doi.org/10.3390/en9040288

Mohapatra, A., Nayak, B., & Saiprakash, C. (2019). Adaptive perturb & observe MPPT for PV system with experimental validation. 2019 *IEEE International Conference on Sustainable Energy Technologies and Systems (ICSETS)*,

Naima, B., Belkacem, B., Ahmed, T., Benbouhenni, H., Riyadh, B., Samira, H., Sarra, Z., Elbarbary, Z., & Mohammed, S. A. (2025). Enhancing MPPT optimization with hybrid predictive control and adaptive P&O for better efficiency and power quality in PV systems. *Scientific Reports*, 15(1), 24559. https://doi.org/https://doi.org/10.1038/s41598-025-10335-0

Renaudineau, H., Donatantonio, F., Fontchastagner, J., Petrone, G., Spagnuolo, G., Martin, J.-P., & Pierfederici, S. (2014). A PSO-based global MPPT technique for distributed PV power generation. *IEEE transactions on industrial electronics*, 62(2), 1047-1058. https://doi.org/https://doi.org/10.1109/TIE.2014.2336600

Saberi, A., Niroomand, M., & Dehkordi, B. M. (2023). An improved P&O based MPPT for PV systems with reduced steady-state oscillation. *International Journal of Energy Research*, 2023(1), 4694583. https://doi.org/https://doi.org/10.1155/2023/4694583

Safari, A., & Mekhilef, S. (2011). Incremental conductance MPPT method for PV systems. 2011 *24th Canadian Conference on Electrical and Computer Engineering (CCECE)*,

Saravanan, S., & Babu, N. R. (2016). Maximum power point tracking algorithms for photovoltaic system–A review. Renewable and Sustainable Energy Reviews, 57, 192-204. https://doi.org/https://doi.org/10.1016/j.rser.2015.12.105

Solís-Cervantes, C. U., Palomino-Resendiz, S. I., Flores-Hernández, D. A., Peñaloza-López, M. A., & Montelongo-Vazquez, C. M. (2024). Design and implementation of extremum-seeking control based on mppt for dual-axis solar tracker. Mathematics, 12(12), 1913. https://doi.org/https://doi.org/10.3390/math12121913

Sonia, P., Aravinda, K., Singla, A., Kumar, Y. J. N., Vishkarma, M. K., Ali, H. A., & Ramu, T. B. (2024). Incorporating Incremental Conductance MPPT Techniques into Solar Power Extraction. *E3S Web of Conferences*,

Tajiri, H., & Kumano, T. (2012). Input filtering of MPPT control by exponential moving average in photovoltaic system. 2012 *IEEE International Conference on Power and Energy (PECon)*,

Tozlu, Ö. F., & Çalık, H. (2021). A review and classification of most used MPPT algorithms for photovoltaic systems. *Hittite Journal of Science and Engineering,* 8(3), 207-220. https://doi.org/https://doi.org/10.17350/HJSE19030000231

Wang, H., Li, L., Ye, H., & Zhao, W. (2024). Enhancing MPPT efficiency in PV systems under partial shading: A hybrid POA&PO approach for rapid and accurate energy harvesting. *International Journal of Electrical Power & Energy Systems*, 162, 110260. https://doi.org/https://doi.org/10.1016/j.ijepes.2024.110260